

Chapter 3

The Relationship Between Arrhenius Pre-factors with Non-Covalent Binding

3.1 Introduction

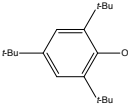
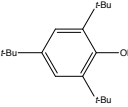
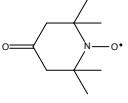
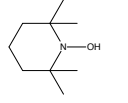
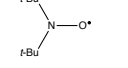
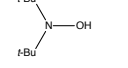
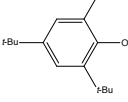
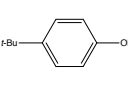
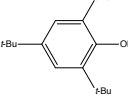
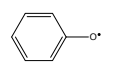
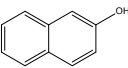
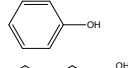
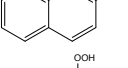
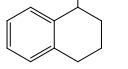
DiLabio and Ingold³⁸ previously investigated the formal HAT reaction of the iminoxyl/oxime self-exchange reaction. In that paper, they compiled a table of parameters from the phenomenological Arrhenius equation for a series of interesting reactions, which appear here in Table 3.1.^{42,129–135} These are thermoneutral hydrogen atom self-exchange reactions involving oxygen-centered radicals, and other nearly thermoneutral reactions involving the destruction and formation of oxygen-centered radicals, reactions 3.1 and 3.2, respectively:



Although it is well known that reactions of this nature involve remarkably low activation energies (E_a),^{136–139} the Arrhenius pre-exponential factors (A), or as they shall be referred to herein, *A-factors*, as well as rate constants, span a wide range (summarized in Table 3.1): The measured *A*-factors range from $10^{3.5}$ – $10^{8.3}$ $\text{M}^{-1}\text{s}^{-1}$ and the rate constants range from 10 – 10×10^7 $\text{M}^{-1}\text{s}^{-1}$. In the past, this range has

3.1. Introduction

Table 3.1: Table of results for (nearly) thermoneutral reactions studied. Units for ΔH , E_a , and calculated pre-reaction complex binding energy (BE) are kcal mol⁻¹, log A are log M⁻¹s⁻¹, and k are M⁻¹s⁻¹. References to the original literature are included with the Complex ID number. [†]Calculated binding energies involve structures that could not be fully optimized and contain one or more small imaginary frequencies. Adapted with permission from Reference 38. Copyright (2005) American Chemical Society.

ID	RO [•] /R'O [•]	ROH	ΔH	log A	E_a	k	BE
1 ⁴²			0.0	3.7	1.2	3.3×10^2	-10.8
2 ¹²⁹			-2.0	3.8	3.8	10	-14.8
3 ⁴²			0.0	5.1	3.5	3.3×10^2	-10.1 [†]
4 ^{130,131}			4.2	5.5	4.8	93	-10.0 [†]
5 ¹³²	$t\text{-BuOO}^\bullet$		-7.0	4.2	0.5	7×10^3	-6.5
6 ⁴²	$\text{Ph}_2\text{NO}^\bullet$	Ph_2NOH	0.0	>7	-	> 10^7	-13.6 [†]
7 ¹³³			-2.2	8.3	2.3	4×10^6	-8.6
8 ¹³⁴	$t\text{-BuOO}^\bullet$		0.3	7.2	5.2	3×10^3	-5.5 [†]
9 ¹³⁴	$t\text{-BuOO}^\bullet$		-1.9	6.4	2.6	3×10^4	-5.6 [†]
10 ¹³⁵	$t\text{-BuOO}^\bullet$		1.4	6.0	4.5	7×10^2	-8.0 [†]

been attributed to steric shielding around the oxygen atoms, resulting in a larger entropic barriers.³⁸ Importantly, it was noted that the degree of steric shielding on the oxygen atom appears to play an important role in the order of the A-factor; systems with greater bulk have lower A-factors, while non-shielded systems have larger A-factors.

3.1. Introduction

Stereo-electronic effects are known to play an important role in HAT, and have been studied extensively.^{40,140–146} Although the abstraction of a specific hydrogen atom may be more thermodynamically favourable than others on a given substrate, if it is not accessible due to steric constraints, abstraction will not occur at this site. Otherwise, additional steric bulk can lead to significant reductions in reactivity, through destabilization of the TS complex, or by forcing additional processes involving conformational changes in order to reach the appropriate TS structure. For example, in reactions of tertiary acetamides with CumO[•],¹⁴⁶ where abstraction occurs mainly from C–H bonds α to the nitrogen atom, a two-fold decrease in the rate constant (normalized for the number of equivalent hydrogen atoms) is observed in going from *N,N*-dimethylacetamide to *N,N*-diisobutylacetamide ($k_H = 2.0 \times 10^5$ and $7.8 \times 10^4 \text{ M}^{-1}\text{s}^{-1}$, respectively). The decrease in rate constant is attributed to the steric clash between the methyl groups of CumO[•] and the isobutyl groups of *N,N*-diisobutylacetamide.

As all of the reactions in Table 3.1 are nearly thermoneutral, thermochemical effects on the rates of reaction are expected to be minimal. Therefore, the large degree of variance in their rate constants (k) is somewhat surprising. These reactions are closely related to the self-exchange reaction between phenol and phenoxyl,²³ in which a strong molecule-radical pre-reaction complex akin to those listed in Table 3.1 is formed, ca. 10 kcal mol⁻¹ below the separated reactants. It is therefore expected that most, if not all, of the systems in Table 3.1 should exhibit a similar molecule-radical complex; granted, the strength of the interaction will vary because of steric repulsion. As such, it is plausible that the strength of this interaction may directly influence the rate of formal hydrogen atom transfer.

Currently, there has been no comprehensive investigation of the relationship between the pre-reaction complex and the kinetics of a reaction. On the basis of

the reaction data in Table 3.1, we ask the question: *Do A-factors have a correlation with non-covalent binding energies of the pre-reaction complex?* This is a reasonable question as non-covalent binding and steric hinderance represent a loss of degrees of freedom and therefore entropy,ⁱ which ultimately determines the A-factor magnitude. If the answer to the question is yes, then non-covalent binding may be useful as a diagnostic for the “looseness” or “tightness” of a TS complex, in addition to providing an important link between theory and experiment.

3.2 Computational methods and details

Density-functional theory (DFT) calculations were carried out using the Gaussian-09 software package.¹¹⁶ Care was taken to obtain minimum energy structures through detailed conformational analysis. For this, the BLYP density-functional^{102,147} was utilized, paired with the empirical D3 dispersion correction¹⁰⁹ with the recommended Becke-Johnson damping functions,¹¹⁰ as well as our groups’ own basis set incompleteness potentials (BSIPs),¹⁴⁸ and minimal MINIs basis sets.¹⁴⁹ The use of minimal basis sets corrected for basis set incompleteness allows DFT-based methods to be used efficiently in performing a large number of calculations. Minimum energy conformers of the monomers (substrates and radicals) were first obtained by manual manipulation of the necessary dihedral bond angles, followed by geometry optimization and vibrational analysis.

The lowest energy radicals and substrates were combined to generate the appropriate pre-reaction complexes. These pre-reaction complexes were subject to conformational analysis using the same BLYP-D3(BJ)-BSIP/MINIs method. Geometries were initially manipulated by hand. It became apparent that manual manipulation

ⁱRecall from Equation 2.95 that the A-factor can be related to TST such that the primary variable is entropy ($\Delta^\ddagger S^\circ$).

resulted in an unsatisfactory exploration of the conformational space. To solve this, all the necessary dihedral angles were scanned systematically using a combination of scripts.¹⁵⁰ All manipulated geometries were subject to optimization. For each complex, the top 5–10 complex geometries were subject to further optimization using a higher level of theory (BLYP-D3(BJ)-BSIP/pc-1) to obtain the final minimum energy pre-reaction complex structures. Due to the free rotation of groups such as *t*-butyl and methyl, some of the optimized pre-reaction complex structures contain small imaginary frequencies, and thus do not represent proper stationary states. Several measures were taken to resolve this, ~~however,~~ no resolution was obtained in many cases. Regardless, the complexes adequately represent the pre-reaction complex and differences in “true” binding energies can likely be ignored.

To obtain accurate pre-reaction complex binding energies, the substrates and complexes were subject to single-point energy calculations using the LC- ω PBE long-range corrected density functional^{151,152} with D3(BJ) dispersion corrections and pc-2 basis sets with *f*-type basis functions removed (pc-2-spd).¹⁵³ This method was selected on the recommendation of work by Johnson et al.¹⁵³, which demonstrated the accuracy of this method for the calculation of NCIs. On the basis of the reported mean absolute error in Reference 153 for the S66 benchmark set of sixty-six different non-covalently interacting dimers,¹⁵⁴ the calculated binding energies reported herein from the LC- ω PBE-D3(BJ)/pc-2-spd level of theory carry an estimated 0.2 kcal mol⁻¹ margin of error.

3.3 Results and discussion

The theoretically determined electronic binding energies calculated for the lowest energy pre-reaction complex of each system are listed in Table 3.1. The logarithm of A-factor against binding energy was plotted, as shown in Figure 3.1. The overall

3.3. Results and discussion

correlation is quite poor ($R^2 = 0.33$), however much of the data is grouped about a single, well correlated line ($R^2 = 0.95$). The intercept of the fitted line that corresponds to zero binding energy is 8.63, a value that is in line with what has been cited as the expected A-factor for HAT reactions, *viz.* $10^{8.5 \pm 0.5} \text{ M}^{-1} \text{ s}^{-1}$.¹⁵⁵ These results suggest that the observed correlation is genuine, that is, NCIs may have an impact on A-factors. I shall demonstrate that the data that do not correlate are reasonable outliers. In fact, using simple rationale I shall demonstrate that different regimes of steric bulk results in different mechanistic processes leading to the TS complex.

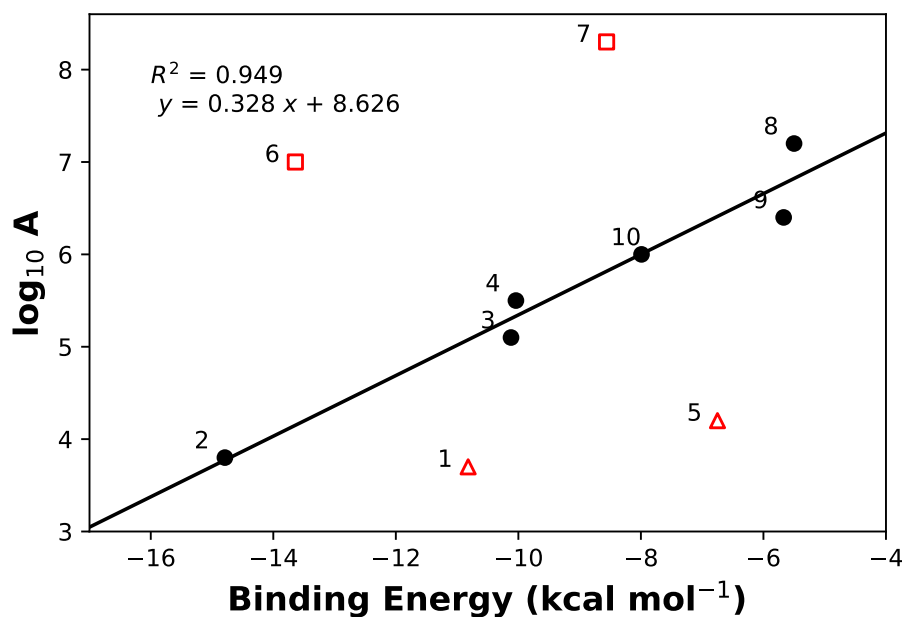


Figure 3.1: Plot of logarithm of A-factor against binding energy. Only the black points were included in the line fitting (slope = $0.328 \text{ kcal mol}^{-1}$, intercept = $8.626 \text{ kcal mol}^{-1}$, and $R^2 = 0.949$). Red points with open faced markers indicate outliers, *vide infra*. The inclusion of complexes 1, 5, and 7 result in an $R^2=0.334$. Complex 6 is always omitted from line fitting as the experimental A-factor is approximate.

In order to understand the deviations from the expected linear trend of A-factor

against pre-reaction complex binding energies, it is important to consider the specific reaction mechanisms taking place. Recall from Chapter 1 that we are focussed on two important possible reaction mechanisms, namely direct HAT and PCET.

For direct HAT to occur, the SOMO of the radical must overlap with the O-H σ^* anti-bonding orbital. In the case of hydrogen abstraction from a phenolic compound, this may require the rotation of the hydrogen atom donating hydroxyl group out of the plane. The rotation of a phenolic hydroxyl group has an energy barrier that follows a $\cos^2 \theta$ relationship.¹⁵⁶ As a reference point, the rotational barrier of phenol¹⁵⁷ is 3.1 kcal mol⁻¹, thus sterically hindered phenols may have a greater rotational barrier. For a PCET mechanism to occur, there are two possible geometries: The nominally singly-occupied O 2p-orbital of the radical ~~overlaps~~ can overlap with the corresponding oxygen LP 2p-orbital, as seen in the work of Mayer et al.²³. Alternatively, a LP- π , LP-LP, or π - π bonding overlap between the radical and substrate can occur, as seen in the work of DiLabio and Ingold³⁸, and DiLabio and Johnson²⁶.

As described in Chapter 1, there remains no clear physical criteria to distinguish direct HAT from PCET, a topic of active discussion in the literature.²²⁻³² One possible solution is consider the existence of these mechanisms ~~exists~~ on a continuum; the rate constant (and thus A-factor) for formal HAT (k_{HAT}) can be described as a combination of the rate constants direct HAT (k_{direct}) and PCET (k_{PCET}) mechanisms, i.e.:

$$k_{HAT} = k_{direct} + k_{PCET} \quad (3.3)$$

Before elaborating on Equation 3.3, we must first discuss the role of the pre-reaction complexes in formal HAT reactions. As a radical and substrate approach sufficient proximity for a reaction to take place, NCIs lead to the formation of a

~~weakly bound~~ weakly-bound complex. If this complex has the appropriate geometry for a hydrogen transfer to occur, it is considered a pre-reaction complex, otherwise it is considered an initial encounter complex. An initial encounter complex must pass over an additional energy barrier to reach the appropriate pre-reaction complex. With respect to the species in Table 3.1, the complexes formed involve various degrees of π - π , LP- π , and LP-LP interactions, which contribute to the weakly attractive, dispersion interactions. Furthermore, these same orbital interactions in the TS complex can lead to the formation of an additional electronic channel, enabling contributions of a PCET mechanism to the overall mechanism.^{26,38} Returning now to Equation 3.3, the different types of orbital interactions may control the contributions of k_{PCET} to the overall rate constants. Our hypothesis, that cannot be tested until a quantitative diagnostic for PCET vs HAT is developed, is that π - π interactions contribute to a PCET dominated mechanism ($k_{HAT} \approx k_{PCET}$). On the other hand, LP-LP interactions are weaker and thus PCET of this nature contributes only weakly to the overall mechanism.

While the data herein explore only the geometries of the pre-reaction complexes involved in the hydrogen transfer reactions, the presumptive TS structures will have similar structures and more importantly, orbital interactions. Therefore, by considering the similarities between pre-reaction and TS complexes, it is possible to rationalize the deviations from the observed trendline in Figure 3.1.

I shall begin by examining the points that fall on the expected line, complexes 2–4 and 8–10. The examination of all these pre-reaction complexes reveals that an additional rearrangement that has a moderate energetic barrier is required in order for the hydrogen transfer to proceed. Complexes 2 and 3 are shown in Figure 3.2, and are very similar in structure. Both are hydroxylamine-nitroxyl couples with similar degrees of steric bulk adjacent to the reacting centres. The *t*-butyl groups of 3, and

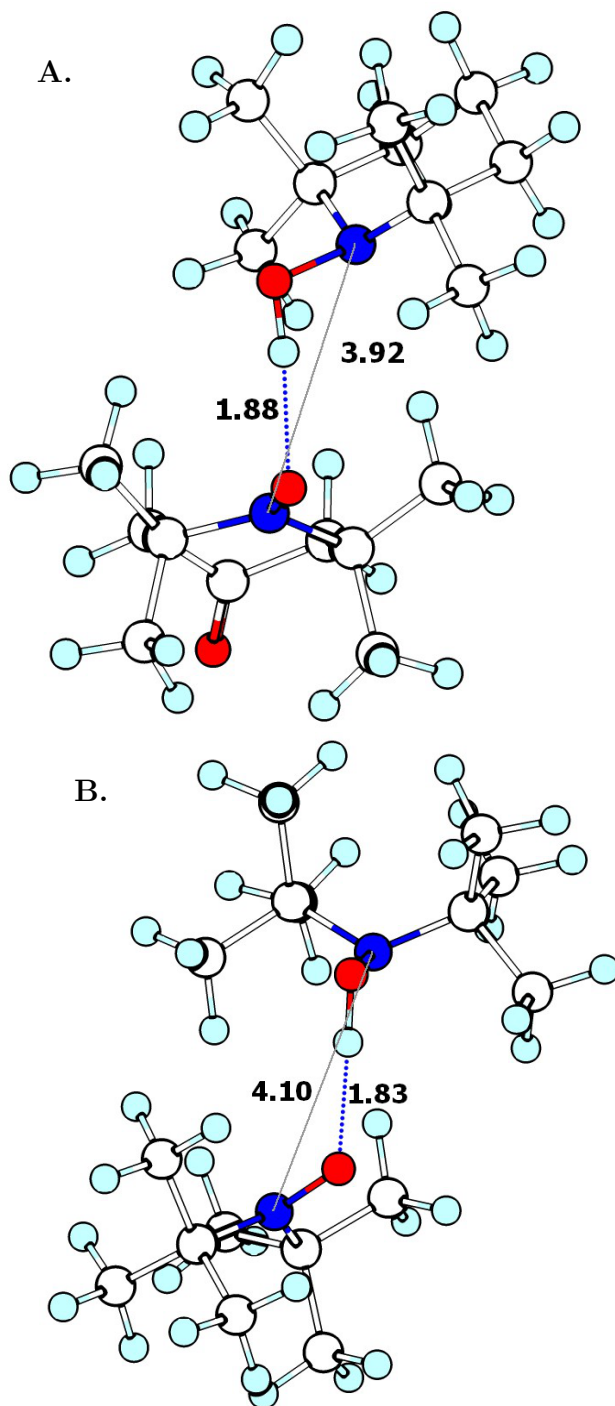


Figure 3.2: Three-dimensional structures of **A** complex 2 (TEMPO-H and 4-oxo-TEMPO) and **B** complex 3 (di-*t*-butyl-hydroxylamine and di-*t*-butyl-nitroxyl). Bond distances are shown in units of Å. The elements are coloured as white for carbon, light blue for hydrogen, red for oxygen, and blue for nitrogen.

3.3. Results and discussion

the methyl groups of **2** (the NO-ON dihedral angles are 65° and 68° , respectively) prevent the overlap of the N LP orbitals in of the NO-H-ON frameworks to allow for PCET. Thus, while the presumptive TS structure may have some degree of LP-LP orbital interaction, the overall mechanism is dominated by direct HAT.

In the most stable stacked conformation, complex **4**, as seen in Figure 3.3, steric clash of the para-position *t*-butyl groups obstructs π - π overlap between the aromatic rings. It is likely that this steric clash does not allow any significant orbital interaction, suggesting that the reaction is dominated by direct HAT. In order to react via direct HAT, the hydroxyl group must rotate ~~further~~ farther out of the aromatic plane, or the bulky para-position *t*-butyl groups must come into close proximity. Alternatively, an open conformation for complex **4** is possible, which lies ca. 2 kcal mol⁻¹ higher in energy than the stacked complex, a result that is also consistent with the observed trend-line. From the open conformation, PCET is still not possible due to the steric bulk of the ortho-position *t*-butyl groups of the radical, thus this reaction likely also proceeds through a direct HAT mechanism. For complex 4, steric clash prevents π - π orbital interactions, therefore the reaction proceeds through a direct HAT dominated mechanism.

Complexes **8** and **9** are similar systems, in which *t*-BuOO[•] reacts with unhindered phenolic substrates. As seen by the structures in Figure 3.4, the bound complexes are somewhat dissimilar. The hydroxyl group of complex **8** is rotated out of the plane 24° , while in complex **9** the hydroxyl group lies entirely in the plane. It is likely that the larger aromatic system of 2-naphthol results in a larger OH rotational barrier, ~~and thus~~. Therefore, the most favourable conformation ~~is for this complex places the phenolic hydroxyl group~~ entirely in the plane. In complex **9**, there is also a weak hydrogen bond between the C-H bond in the ortho-position and the non-radical O-centre of *t*-BuOO[•], contributing further to the stabilization of

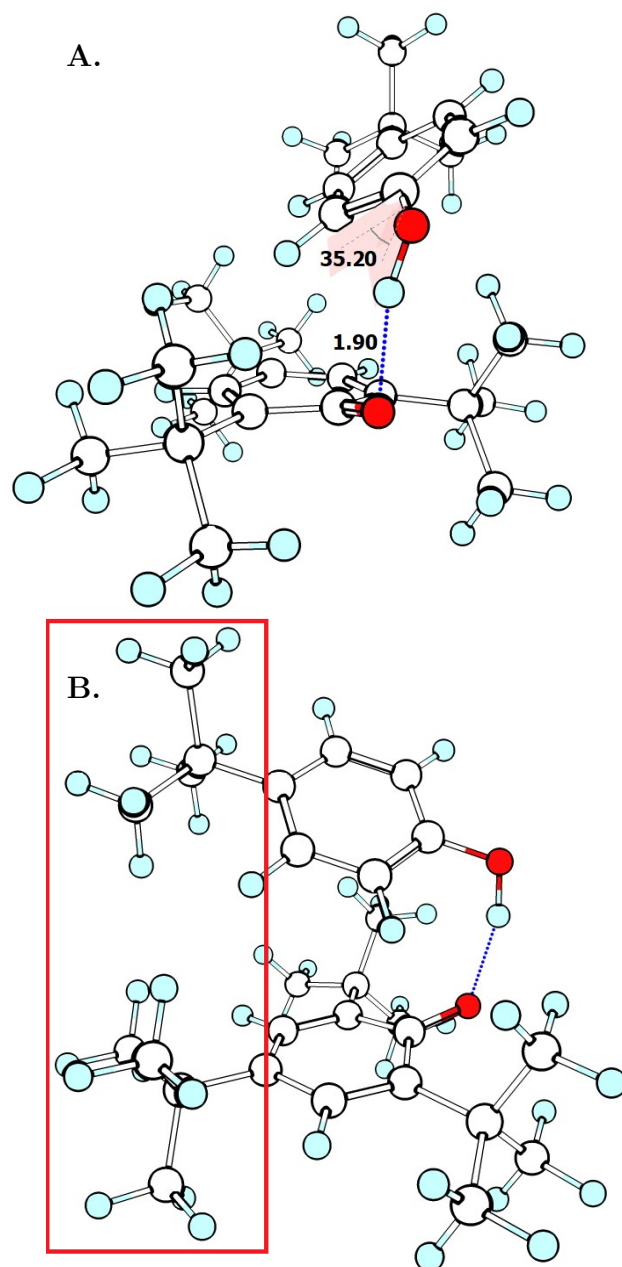


Figure 3.3: Three-dimensional structure of pre-reaction complex 4 between 2,4,6-tri-*t*-butylphenol and 4-*t*-butylphenoxy. **A** demonstrates the hydrogen bond distances in units of Å, and the out-of-plane rotation by 35.2° of the phenolic hydroxyl group. **B** demonstrates the steric clash (highlighted by red box) between the para-position *t*-butyl groups. The elements are coloured as white for carbon, light blue for hydrogen, and red for oxygen.

3.3. Results and discussion

the planar conformation. Complex 8 was previously studied by DiLabio and Johnson²⁶, where it was demonstrated that a partial bonding interaction exists between the peroxy LP and phenolic π -system in the TS complex. However, this interaction is likely weak and thus contributes weakly to the overall rate constant. That is, k_{HAT} is dominated by k_{direct} . Also, although the pre-reaction complexes are somewhat dissimilar, the conformational changes necessary to reach the TS complex, similar to that reported in reference 26, are likely not dramatically different in terms of energetic barriers. Any small differences result in noise in the observed trend.

Complex 10, shown in Figure 3.5 is unique in that it is the only reaction between a peroxide and a peroxy radical. Therefore, this system represents the best case scenario for LP-LP overlap to occur. The self-exchange reaction between HOO^\bullet and HOOH can be considered the simplest reference for the reaction of α -tetralin peroxide with *t*-butylperoxy. To the best of my knowledge, the mechanism of the hydroperoxyl-hydrogen peroxide couple has not been characterized as either PCET or direct HAT previously in the literature, although the TS structure has been previously reported.¹⁵⁸ Using this structure, calculations reveal a LP-LP interaction leading to partial bonding in the TS, i.e. a PCET mechanism. (See Appendix A, Figure A.1). The hydroperoxyl-hydrogen peroxide couple contains a H–O–O–H dihedral angle of 90° , so that the two non-reacting hydrogen atoms oriented 180° away from one another. Orienting substituents directly away from one another is likely the most stable TS structure for all peroxy-peroxide formal HAT reactions.

~~Complex 10 is unlikely to orient~~ The orientation of *t*-butylperoxy and α -tetralin peroxide at exactly 180° away from one another is unfavourable in complex 10, due to steric clash. Nonetheless, there may still be some LP-LP overlap contributing to a weak k_{PCET} contribution to k_{HAT} . On the basis of ~~the line fit in Figure 3.1,~~

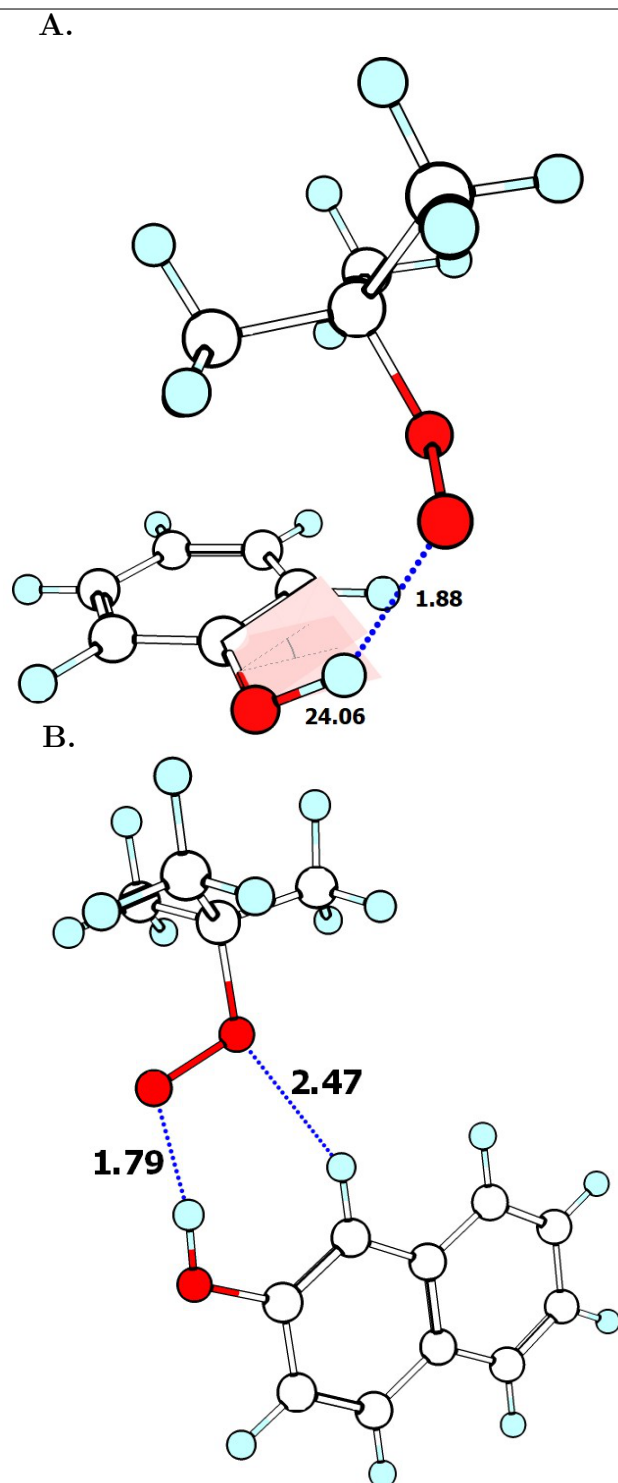


Figure 3.4: Three-dimensional structures of pre-reaction **A** complex 8 (*t*-butylperoxyl and phenol) and **B** complex 9 (*t*-butylperoxyl and 2-naphthol). Bond distances are shown in units of Å. Complex 8 has an out of plane rotation of the phenolic hydroxyl group of 24.1° . The elements are coloured as white for carbon, light blue for hydrogen, and red for oxygen.

3.3. Results and discussion

~~and given that the other point are dominated by k_{direct} , the same is likely true in the case of complex 10. This means that either the TS structure does not allow for sufficient our hypothesis, LP-LP overlap for k_{PCET} to dominate, or LP-LP overlap does interactions do not allow for ~~a strong PCET contribution to k_{HAT}~~ PCET to contribute strongly to the overall mechanism. This will require additional investigation. For complex 10, k_{HAT} is dominated by k_{direct} .~~

Once again, complexes 2–4 and 8–10 follow the observed trend. In all cases, these complexes may have some PCET contribution to k_{HAT} through either LP- π or LP-LP orbital overlap. Interpretation of Figure 3.1 in this manner allows for two possible explanations. The simplest is that all these complexes proceed through a mechanism in which $k_{HAT} \approx k_{direct}$ ($k_{PCET} \ll k_{direct}$). In this case, the A-factor is a direct reflection of k_{HAT} and this the pre-reaction complex binding energy correlates well with the A-factor.

Alternatively, there may be increasing contributions of PCET leading to an increase in the A-factor. This effect can be rationalized on the basis of a stronger interaction in the case of LP- π overlap, as compared to LP-LP overlap. Within this framework, complexes 2, 3, and 4 may have little or no overlap due to steric clashing, and complexes 8 and 9 have a higher A-factor than complex 10 due to LP- π vs. LP-LP overlap. Further work is necessary to discern this effect.

Consider next the points that sit above the trendline, complexes 6 and 7, shown in Figure 3.6 and Figure 3.7. The A-factor for complex 6 is approximate and thus does not get factored into the line fitting. In both cases, the non-covalently bound complexes are in a slipped-parallel π -stacked conformation, allowing for π - π orbital overlap. Complex 7 in particular is very similar to the phenol-phenoxy couple, except with 2-naphthol instead of phenol. In both cases, the π -stacked pre-reaction complex is very close to the presumptive TS structure. Therefore, it is possible to

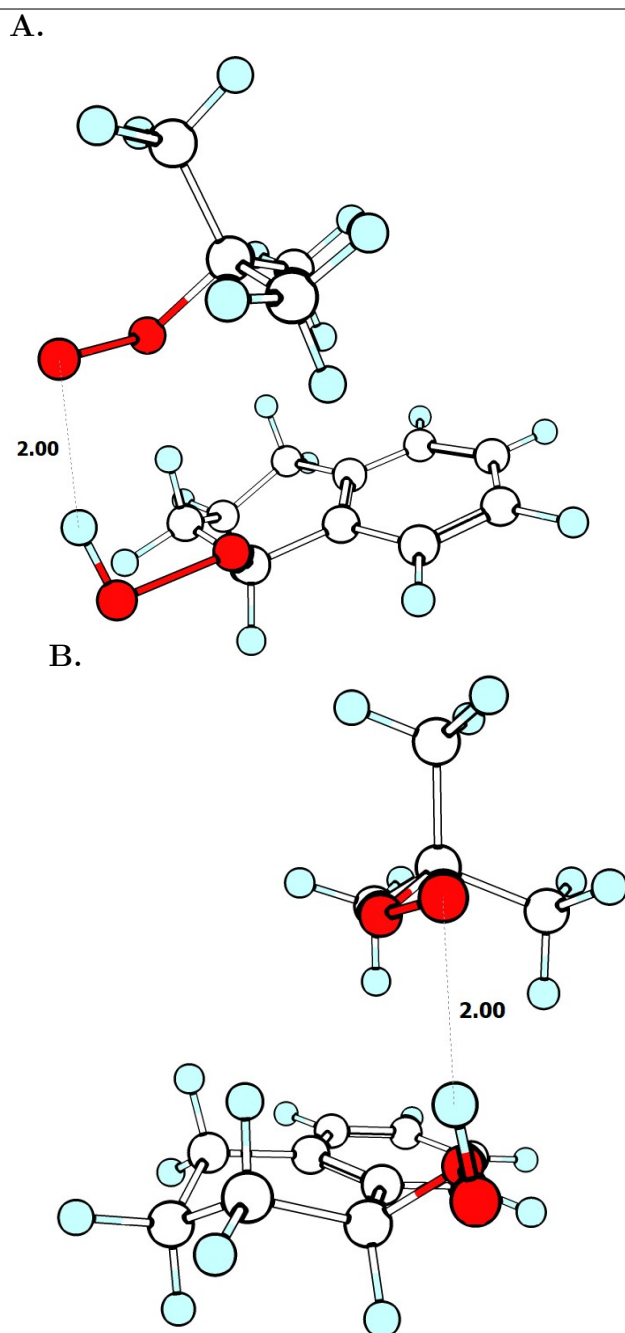


Figure 3.5: Three-dimensional structure of pre-reaction complex 10 between *t*-butylperoxyl and α -tetralin peroxide. **A** demonstrates the hydrogen bond distances in units of Å. **B** demonstrates the likely steric clash preventing strong LP-LP overlap. The elements are coloured as white for carbon, light blue for hydrogen, and red for oxygen.

3.3. Results and discussion

infer that both of these reactions take place through mechanism in which k_{PCET} is dominant. The key difference from the points that fall on the trendline is that $k_{HAT} \approx k_{PCET}$.

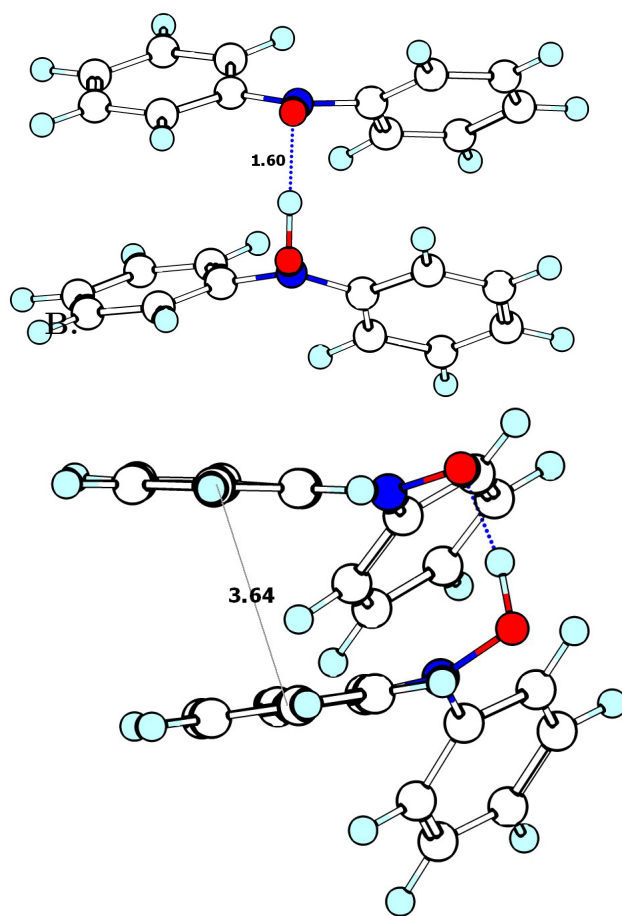


Figure 3.6: Three-dimensional structures of pre-reaction complex 6 between *N,N*-diphenylhydroxylamine and *N,N*-diphenylnitroxyl. **A** demonstrates the hydrogen bonding interaction while **B** demonstrates the π - π interaction. Distances in unit of Å and angles are shown in degrees. The elements are coloured as white for carbon, light blue for hydrogen, blue for nitrogen, and red for oxygen.

Lastly, consider the points that fall below the trendline, complexes 1 and 5. In both cases, a high degree of steric repulsion likely does not allow for a PCET mech-

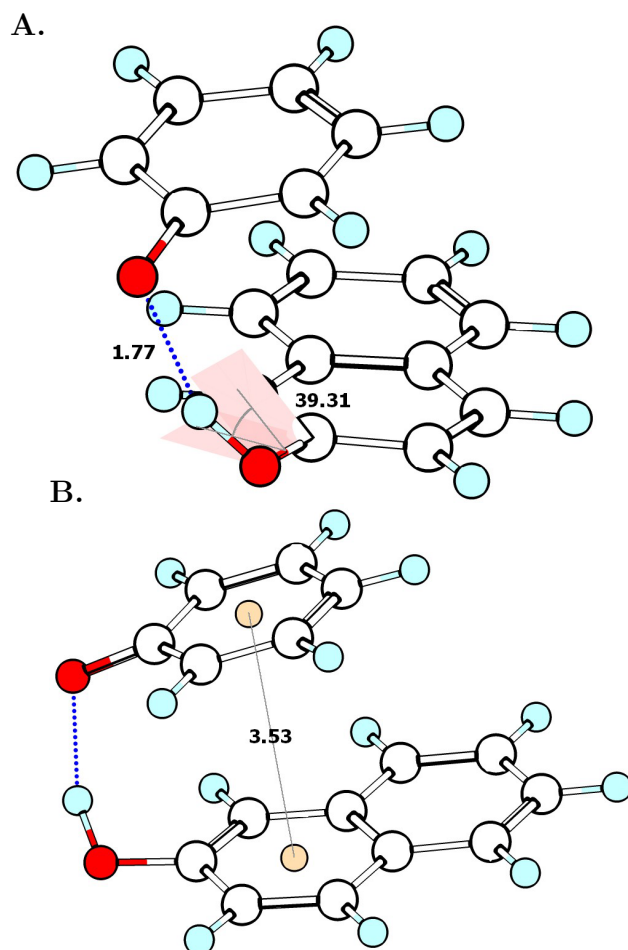


Figure 3.7: Three-dimensional structures of pre-reaction complex 7 between 2-naphthol and phenoxy. **A** demonstrates the hydrogen bonding interaction while **B** demonstrates the π - π interaction. Distances in unit of Å and angles are shown in degrees. The elements are coloured as white for carbon, light blue for hydrogen, and red for oxygen.

anism through orbital overlap. It is important to study the “encounter complex” that represents the first pre-reaction complex, i.e. prior to any reorganization, as this will be the complex that affects the A-factor with regards to simple collision theory. Complex 1 is the self-exchange reaction between the very bulky 2,4,6-tri-*t*-butylphenol/2,4,6-tri-*t*-butylphenoxyl couple, as seen in Figure 3.8 A. As a result of steric shielding around the reaction centres, the encounter complex is stacked to maximize dispersion interactions, but does not have a hydrogen bond. Therefore, an additional rearrangement is required in order to get to the presumptive TS structure. That is, there must be a higher-energy hydrogen-bonded pre-reaction ~~couple~~ complex that leads to the direct HAT mechanism. Note however, that there is a barrier to rotation of the hydroxyl group to 90° out of the plane for direct HAT to occur.

Complex 5 is the 2,4,6-tri-*t*-butylphenol/*t*-butylperoxyl reaction couple. The encounter pre-reaction complex also does not contain a hydrogen bond. As with complex 1, an encounter complex without a hydrogen bond must form first. However, in complex 5 there is less steric clashing. As a result the formation of a hydrogen bond is favourable and the “true” pre-reaction complex is about 0.7 kcal mol⁻¹ more stable than the encounter complex. In contrast, for complex 1 the true pre-reaction complex is about 0.6 kcal mol⁻¹ less stable than the encounter complex. Note also that there is a barrier to rotationⁱⁱ of the hydroxyl group that can be estimated as about 4.1 kcal mol⁻¹. This is illustrated schematically in Figure 3.9.

For both complex 1 and 5, steric clashing prevents significant π - π overlap or LP- π overlap. Therefore, the reactions likely proceed through a direct HAT dominated mechanism ($k_{HAT} \approx k_{direct}$). One might then expect these data to fall on the trendline, however the formation of an encounter complex that does not lead directly

ⁱⁱCalculated as the difference in energy between the in-plane and out-of-plane structures of 2,4,6-tri-*t*-butylphenol at the LC- ω PBE-D3/6-311+G(2d,2p) level of theory.

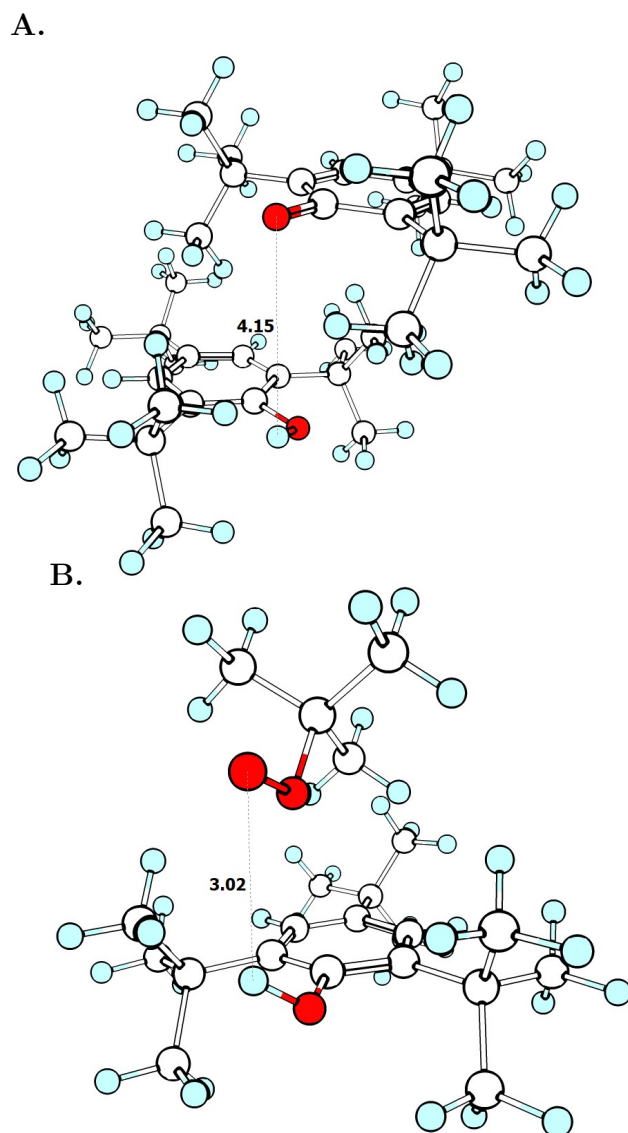


Figure 3.8: Three-dimensional structures of pre-reaction **A** complex 1 (2,4,6-tri-*t*-butylphenoxl and 2,4,6-tri-*t*-butylphenoxyl) and **B** complex 5 (2,4,6-tri-*t*-butylphenol and *t*-butylperoxyl). Distances in unit of Å and angles are shown in degrees. The elements are coloured as white for carbon, light blue for hydrogen, and red for oxygen.

3.4. Summary

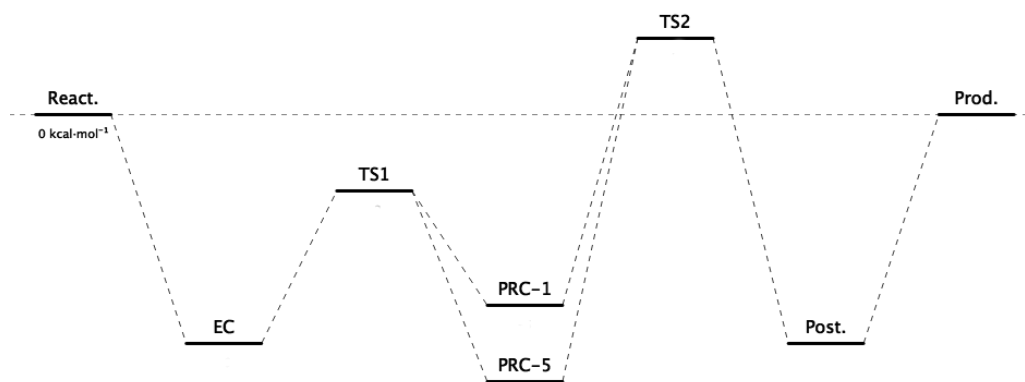


Figure 3.9: Reaction coordinate qualitatively illustrating the proposed mechanism for HAT in complexes 1 and 5. React. = reactants, EC = encounter complex, PRC-1/5. = true pre-reaction complex 1/5, TS1 = transition state associated with out-of-plane rotation of the OH group, TS2 = (presumptive) TS associated with HAT, Post. = post-reaction complex, Prod. = products.

to HAT results in a different overall process from the other complexes. As a result of the necessary initial process complex 1 and 5 have lower A-factors as ~~less~~ fewer collisions are likely to lead to successful formal HAT.

3.4 Summary

In this investigation, a series of thermoneutral or nearly thermoneutral HAT reactions were considered. I have plotted the logarithm of experimentally determined A-factors against the theoretically determined electronic binding energies. These results demonstrate that the A-factors for (nearly) thermoneutral HAT reactions correlate to some extent with the pre-reaction complex binding energies, given that the reactions proceed through similar mechanisms and energetically similar pathways. The results herein can be sorted into three bins by considering the contributions of k_{direct} and k_{PCET} to the overall transformation, k_{HAT} :

1. Complexes that have weak k_{PCET} contributions due to either LP-LP or LP- π

3.4. Summary

orbital overlap, and are therefore dominated by k_{direct} . This is the case for the data that fall on the trendline.

2. Complexes in which k_{PCET} is the dominant contribution to k_{HAT} , as is the case for complexes 6 and 7.
3. Complexes in which the encounter complex does not lead directly the HAT TS complex, as was the case for complexes 1 and 5.

These results indicate that different regimes of electronic and steric interactions lead to different chemical processes in seemingly similar reactions. As a results, non-covalent binding can be used as a metric for kinetics parameters, however, it cannot describe in full the entropic factors that contribute to the A-factor. One must first consider the mechanistic details in which formal HAT occurs.

Additional work is necessary to extend these results. In particular, the main question that remains is whether π - π PCET is “better” than other forms of orbital overlap. To answer this a larger sample of data points, and a diagnostic for PCET must be used. Regardless, the results herein represent a novel attempt to link theory and experiment. Given that obtaining the full PES for large molecules is currently computationally impractical, these results serve as a seed for developing a fundamental understanding of complex formal HAT reactions.